A New Focus on Groundwater–Seawater Interactions
(Proceedings of Symposium HS1001 at IUGG2007, Perugia, July 2007). IAHS Publ. 312, 2007.

Nutrient inputs through submarine groundwater discharge to Ariake Bay, Kyushu Island, Japan

JUN YASUMOTO[1], MAMORU KATSUKI[1], HIDETOMO TAKAOKA[2], YOSHINARI HIROSHIRO[1] & KENJI JINNO[1]

1 *Institute of Environmental Systems, Graduate School of Engineering, Kyushu University, 744 Motooka Nishi-ku, Fukuoka 812-8581, Japan*
yasumoto@civil.kyushu-u.ac.jp

2 *IDEA Consultants Inc., 1-5-12 Higashihama Higashi-ku, Fukuoka 812-0055, Japan*

Abstract Submarine groundwater discharge (SGD) is now recognized as an important pathway between land and sea. This study attempts to estimate the nutrient inputs through SGD to Ariake Bay. SGD rates and its quality along the coast of Ariake Bay in the Oura Region, Japan, were investigated. It was shown that the on-site SGD rate ranges from 0.01 to 20.52 μm/s, and SGD flows through the shallow confined aquifers, which consist of two kinds of rocks: basalt and pyroclastic rocks. The reduction reaction for SGD proceeded just up to denitrification. SGD associated with nutrient loads of N, P and SiO_2 were estimated to be 1.40, 0.07 and 52.78 g m^{-2} d^{-1}, respectively. This study demonstrates that SGD must be considered as a significant source of nutrient input to the coastal sea area in Ariake Bay.

Key words submarine groundwater discharge; nutrient; redox reaction; field survey; seepage meter; Japan

INTRODUCTION

The ecosystem and aquatic environment for human activities and fisheries in semi-enclosed bays as well as coastal areas have been deteriorating in recent years. This study focuses on the environmental reclamation of Ariake Bay, a semi-enclosed inner bay located to the west of Kyushu Island, Japan, which is experiencing such problems. Although the government has implemented several measures to improve the ecosystem and aquatic environment, significant recovery has not yet been achieved in the bay. One of the causes of the deteriorating situation is considered to be an increase in the nutrient flux, due to fertilizers and wastewater, through continuous surface water and groundwater discharges from the residential and agricultural areas into the Ariake Bay catchment.

In recent studies, it has been revealed that nutrient discharge through submarine groundwater discharge (SGD) is not negligible as compared to river discharge (Taniguchi *et al*., 2002). Nutrient discharge plays a significant role in the nutrient cycle and primary productivity in the coastal ocean (Slomp & Van Cappellen, 2004).

In the case of Ariake Bay, however, there is only a little quantified information of whether SGD is the nutrient source. A detailed investigation of SGD and nutrient transport via SGD is indispensable for a better understanding of the role of SGD and its anthropogenic or natural perturbations. This paper takes a first step at estimating nutrient inputs through the SGD to the coast of the Saga region of Ariake Bay by seepage meter measurements.

STUDY SITE AND METHODS

Geography and geology

The study site is off the Oura coast, Tara-town in Saga, which is located on the west coast of Ariake Bay, Kyushu Island, Japan. The SGD observation points (St.1, St.2, St.3, St.4) and groundwater observation points (St.A, St.B, St.C, St.D) in the land region are as shown in Fig. 1.

The Taradake area, as shown in Fig. 2, has a topography dominated by Tara-dake Mountain, with the highest peak 1075 m in elevation and a base of 25 km in diameter. The volcano-foot alluvial fan with a gentle slope of 3–4° develops to the foot of a mountain in the northeast. In the southern area, there are a lot of small rivers which radiate from the central part of the area.

Aquifers in this study area consist of Pliocene to early Quaternary volcanic rocks which are listed chronologically, divided into six stratigraphic units: pre-Taradake andesite (PTA), Taradake Older basalts (TOB), Koorigawa volcanic rocks (KVR),

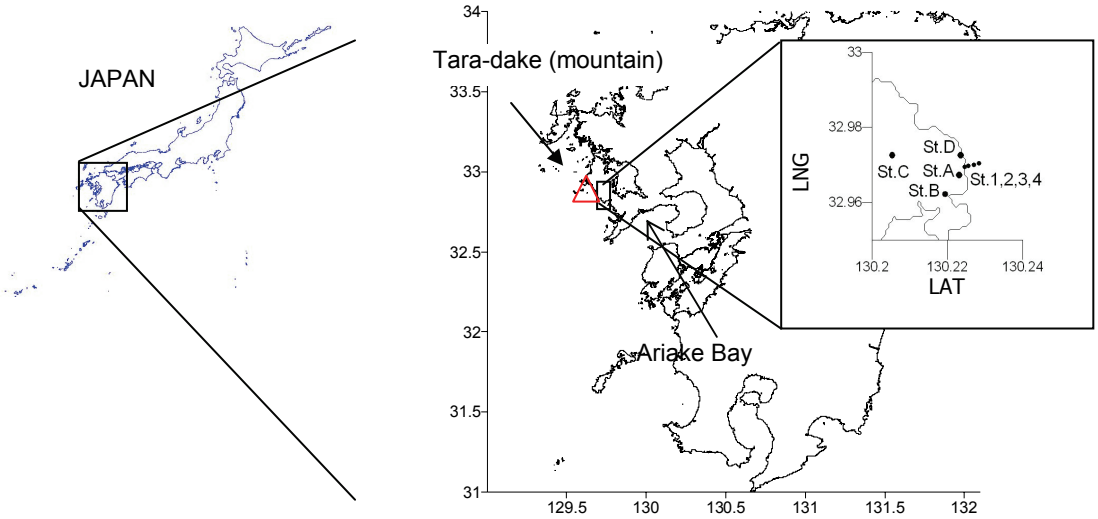

Fig. 1 Location map of Ariake Bay and the study sites.

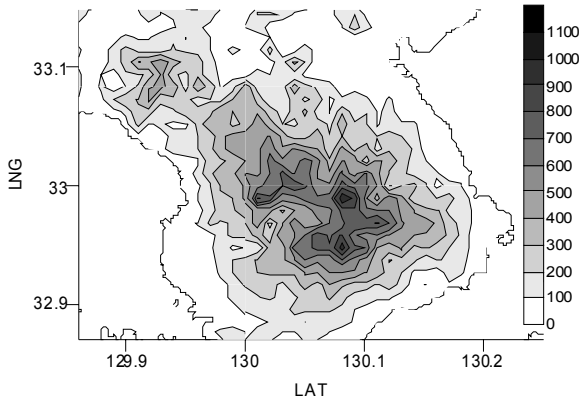

Fig. 2 Topography and geography of the Taradake area.

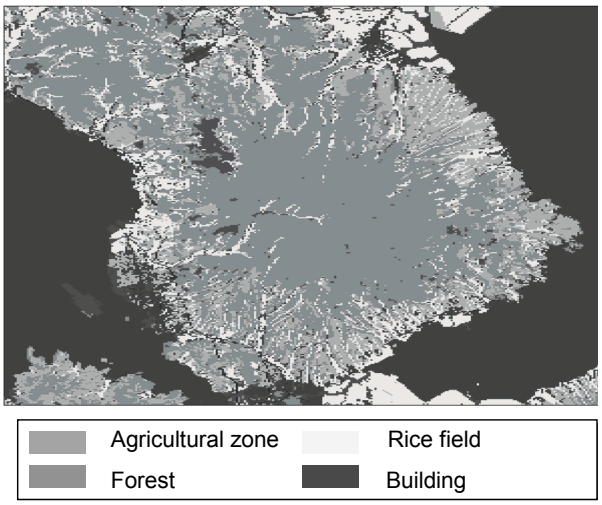

Fig. 3 Use of the land in the Taradake area.

Taradake Older andesites (TOA), Taradake Younger basalts (TYB) and Taradake Younger andesites (TYA). TOB is widely distributed in the base part of Taradake area and is widely exposed to the basement of the mountains except at the southern part. It forms an extensive lava plateau with an area of 15 × 25 km and thickness of 100–250 m. This is one of several large basalt plateaus in the northwestern Kyushu. TOB consists mainly of lava flows with a relatively small amount of pyroclastic rock. The thickness of the lava flow layer is about 30 m. Cracks have developed resulting in high permeability. In contrast, the pyroclastic rock, consisting of volcanic ash and a scoria layer, which consists in many cases of reddish brown clays because of weathering, and has low-permeability.

Figure 3 shows the land use in the Taradake area where there are many agricultural zones at the base of the mountain, which are below 300 m in elevation. The agricultural zones are chiefly used for orange grove cultivation.

The schematic cross-sectional image of SGD in the study area was made based on the geography-topography and geology described above as shown in Fig. 4. It was inferred that the groundwater discharges via a relatively short route through the confined aquifer between the pyroclastic rock with low-permeability and lava flow with high permeability that are formed in the TOB under the sea floor off the coast.

Investigation methods and water analysis items

Ariake Bay is a semi-closed bay, and the average of the tidal change is from 3 to 5 m. Lee-type seepage meters were installed at about 200 m offshore from the coast line. The principles of the Lee-type seepage meter are described in detail by Lee (1977). The seawater depths at high tide are 5.3, 6.4, 6.4, 6.9 m at seepage meters St.1 (20 m offshore), St.2 (35 m offshore), St.3 (100 m offshore) and St.4 (200 m offshore), respectively.

Measurements of the SGD flux and water sampling using the Lee-type seepage meter of 32 cm in diameter were undertaken four times at flood tide (FT), high tide (HT), ebb tide (ET) and low tide (LT) during the one tidal cycle between 20 and 21

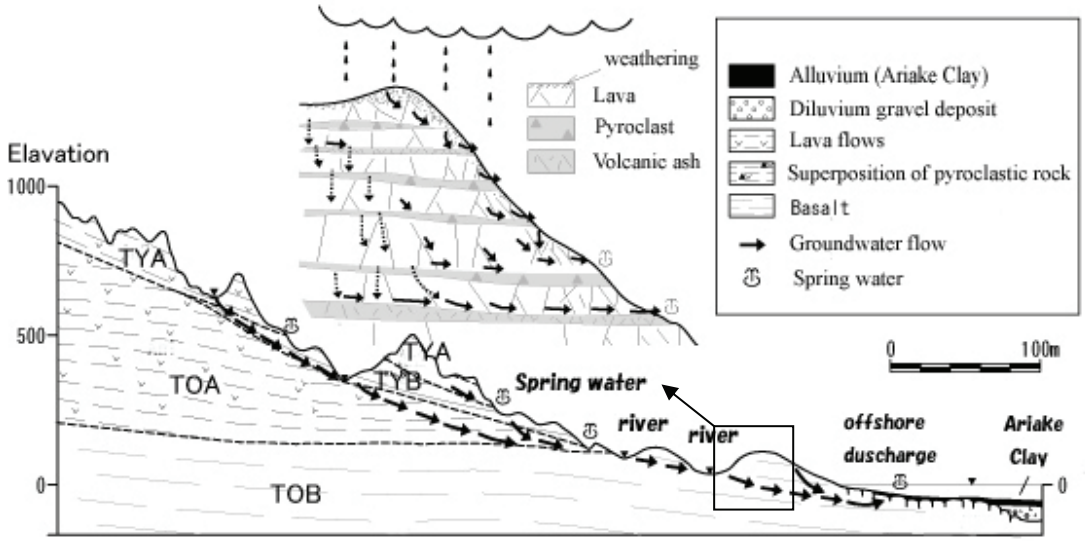

Fig. 4 Schematic cross-sectional image of SGD in the Tara area, Saga, Kyushu Island, Japan.

Table 1 Tidal conditions during the field survey (HT: high tide, LT: low tide).

Date	Sea level: Mean sea level of Tokyo Bay（time, h）	Tide range
20 August 2006	LT –1.22 m（13:05）~HT 1.4 m（19:49）	2.63 m
21 August 2006	HT 1.76 m（7:31）~LT –1.48 m（13:57）	3.24 m

August 2006 (Table 1). Moreover, groundwater sampling was done at four points (St.A, St.B, St.C, and St.D) in the coastal region. The sampled water at St.A and St.D represents groundwater discharge from the slope in the vicinity of the observation point of the SGD. St.B is a deep well in the confined aquifer whereas St.D is a disused artesian well about 5 m from ground level.

The chemical components of water samples of SGD, groundwater and seawater were analysed. Water temperature, electrical conductivity (EC), pH, dissolved oxygen (DO), and oxidation–reduction potential (ORP) of water samples were measured in the field using portable meters. Water quality analysis comprised dissolved organic carbon (DOC), total organic carbon (TOC), major ions (cations: Na^+, K^+, Ca^{2+}, Mg^{2+}, Fe^{2+}, Mn^{2+}; anions: Cl^-, HCO_3^-, SO_4^{2-}), nutrients (ammonium-nitrogen: NH_4^--N; nitrate-nitrogen: NO_3^--N; nitrite-nitrogen: NO_2^--N; phosphate: PO_4^{2-}-P), and the ratio of stable isotopes of hydrogen and oxygen (δD:$\delta^{18}O$).

RESULTS AND DISCUSSION

The primary factors controlling the flux of nutrients through coastal aquifers and sediments into coastal waters are the flow paths and rates of the groundwater, since these factors affect the residence time and contact time of the groundwater with the aquifer solids. If the redox potential of groundwater is low then N and P will be strongly affected. Therefore, the analysis of the SGD paths and rates and the evaluation of the

nutrient flux affected by the reduction reaction processes are highlighted in the present study.

SGD rates and paths

SGD occurs in response to hydraulic connection and sufficient potential gradient between either the shallow or the deep coastal aquifers and the sea. SGD can be mainly found along the shoreline, or sometimes offshore (Slomp & Van Cappellen, 2004).

The observed SGD rates and EC at each observation point and under each tidal condition are shown in Table 2. From the measurements made by the seepage meter, large SGD rates were observed at St.1 and St.2. Specifically, the observed average SGD rate at St.2 ranged from 24.23 to 15.78 μm/s (average: 25.52 μm/s), while the EC was 32 mS/m, which was close to the freshwater value. On the other hand, the average observed SGD at St.1 was 0.76 μm/s, and the average EC was 2823 mS/m, which was almost half-way between those of freshwater and seawater. There was a small amount of SGD at St.3 and St.4; however, EC was very close to the seawater value, which implies that the measured SGD may contain seawater. This implies that the measured SGD at these points may be contaminated by seawater, suggesting that the SGD might be composed of both fresh groundwater originating from the land region and possible seawater in the aquifer, which has recirculated between the sea and the marine sediment.

Figure 5 shows the distribution of submarine fresh groundwater discharge (SFGD), which is calculated using equation (1) and the measured SGD rates. Equation (1) expresses the mixture ratio of the seawater included in the measured SGD (Taniguchi *et al*., 2002).

$$q_{SFGD} = \frac{EC_{SGD} - EC_{GW}}{EC_{SW} - EC_{GW}} \cdot q_{SGD} \tag{1}$$

where q_{SGD} is submarine groundwater discharge rate, q_{SFGD} is submarine fresh groundwater discharge rate, EC_{SGD}, EC_{GW}, EC_{SW} are the electric conductivity of SGD, groundwater at the coast region, and seawater at 200 m offshore (St.4), respectively.

The SGD and the SFGD observed at St.2 were almost the same, and the SFGD rate increased at low tide (Table 2). The SFGD component of the measured SGD was 99.6% at St.2, and the evidence of mixing of seawater could be hardly seen. On the

Table 2 The measured SGD rate (μm/s) and EC (mS/cm) (FT: flood tide, HT: high tide, ET: ebb tide, LT: low tide).

Point	Item	Tidal conditions			
		FT	HT	ET	LT
St.1	Rate	1.14	0.36	0.73	0.83
	EC	3155	2815	2695	2625
St.2	Rate	15.78	20.03	22.04	24.23
	EC	27	36	43	21
St.3	Rate	0.18	0.34	0.23	0.31
	EC	3920	3965	4120	4020
St.4	Rate	0.26	0.49	0.13	0.26
	EC	4215	4070	4390	4015

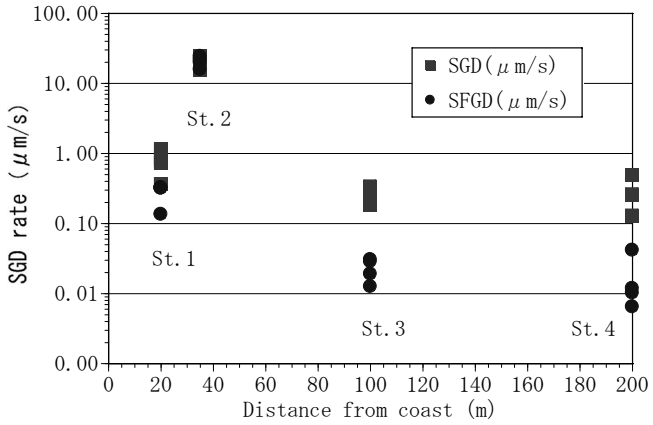

Fig. 5 Distribution of SGD and SFGD rates.

other hand, the SFGD component of the measured SGD at St.1, St.3 and St.4 was 39.4, 8.6 and 5.9%, respectively. The results also suggest that the SGD rate essentially increased from the shoreline to the offshore, but locally considered as a very large value. The SGD through locally developed cracks in the offshore submarine aquiclude from the shallow confined aquifer which consists of the pervious rock (basalt) and aquiclude (pyroclastic rock).

Nutrient fluxes affected by reduction reaction processes

It is important to understand the redox environment of the subsurface in addition to the rates and paths of SGD, since the nutrient transport to the coastal ocean as SGD could be affected by the reduction reaction processes.

Shallow pristine aquifers with short residence times (high recharge and flow rates) and low soil water DOC concentrations may remain largely oxidized. In shallow or deep (intermediate or regional aquifers) with longer residence time and/or higher DOC inputs, dissolved oxygen is usually entirely consumed and organic matter decomposition proceeds via denitrification, Mn and Fe oxide reduction, sulfate reduction and, ultimately, methanogenesis (Lovely & Chapelle, 1995). As a result, the aquifer becomes progressively more reduced toward the direction of groundwater flow (Murphy & Schramke, 1998).

The results of water quality analysis indicate the difference in ORP between the SGD (ORP = 193 mv) and groundwater in the coastal region (ORP = 209 mv), as shown in Table 3. This shows that the SGD is characterized by relatively reductive conditions as compared with the groundwater in the coastal region. Meanwhile, the average NO^{3-}-N concentration in the SGD was 0.75 mg/L, which was low compared to the upstream groundwater (2.44 mg/L). Several studies have shown that a decrease in NO_3^--N concentration in groundwater can be attributed to biochemical denitrification processes (Hill *et al*., 2000). The reaction formula of this process is:.

$$4NO_3^- + 5C + 3H_2O = 2N_2 + 5HCO_3^- + H^+ \quad (2)$$

Denitrification is the biochemical nitrate reduction, which occurs only in a reduction condition with sufficient organic compounds. Table 3 shows that the HCO_3^-

Table 3 The results of water quality analyses.

Item	Unit	SGD:FT (St.2)	SGD:HT (St.2)	SGD:ET (St.2)	SGD:LT (St.2)	GW (St.A)	GW (St.B)	GW (St.C)	GW (St.D)	SW (St.4)	SW (St.4)
TP	C°	26.9	26.7	26.6	26.8	26.4	26.3	26.4	26.4	26.3	26.4
pH	-	8.2	8.1	8.2	8.1	7.2	8.0	7.4	7.5	7.6	7.7
EC	mS/m	16.9	42.1	22.0	24.7	9.3	11.8	19.4	15.5	3820	3650
DO	mg/L	9.8	9.6	8.7	9.9	9.2	8.8	9.4	9.5	5.9	7.1
ORP	mV	196	192	193	191	213	206	210	208	186	185
DOC	mg/L	0.1	0.2	0.2	0.1	0.2	0.1	0.3	0.1	1.1	1.3
TOC	mg/L	0.2	0.2	0.2	0.2	0.9	0.5	0.9	0.1	1.1	1.3
Na^+	mg/L	17.4	58.3	25.4	30.0	6.4	5.6	13.3	11.7	9310	8240
K^+	mg/L	6.4	5.4	4.0	4.1	1.2	1.6	1.7	1.8	382	358
Ca^{2+}	mg/L	7.6	9.1	8.4	8.8	5.5	11.0	14.8	9.4	466	418
Mg^{2+}	mg/L	4.9	8.5	4.6	5.1	2.4	3.5	4.7	4.7	1040	940
Fe^{2+}	mg/L	0.05	ND	ND	ND	0.09	ND	ND	ND	1.27	1.22
Mn^{2+}	mg/L	0.006	ND	ND	ND	0.027	ND	ND	ND	0.514	0.542
Cl^-	mg/L	18.0	94.2	34.1	42.6	11.6	6.2	21.4	11.2	16700	15800
HCO_3^-	mg/L	52.8	50.5	49.2	49.1	19.1	44.6	31.9	44.1	79.7	80.3
SO_4^{2-}	mg/L	4	16	6	7	2	2	7	6	2500	2300
NH_4^+	mg/L	ND	ND	ND	ND	0.06	ND	ND	0.06	ND	ND
NO_3^-	mg/L	0.75	0.75	0.75	0.75	0.32	1.27	5.31	2.88	0.13	0.10
NO_2^-	mg/L	0.002	0.002	0.002	0.002	0.001	0.002	0.001	0.002	0.026	0.019
TN	mg/L	0.79	0.79	0.79	0.80	0.43	1.31	6.15	3.14	0.69	0.63
PO_4^{2-}	mg/L	0.037	0.041	0.040	0.040	0.016	0.046	0.030	0.036	0.043	0.042
TP	mg/L	0.040	0.043	0.042	0.042	0.062	0.048	0.048	0.038	0.116	0.092
SiO_2	mg/L	31	31	27	29	15	24	46	25	4	4

ND: no detection; SGD: submarine groundwater discharge; GW: groundwater; SW: seawater; FT: flood tide; HT: high tide; ET: ebb tide; LT: low tide; WT: water temperature.

concentrations in the SGD were higher than those of the upstream groundwater, while low TOC was observed in the SGD compared to the shallower groundwater. However, a significant difference in the concentration of $Mn^{2+}$and Fe^{2+} was not seen between SGD and the upstream groundwater. The SGD shows a higher concentration of SO_4^{2-} compared to the upstream groundwater. Similarly, Cl^- concentration in the SGD was higher than in the upstream groundwater. Therefore, it can be assumed that this phenomenon occurred due to the mixing of seawater. The relationship between the SGD and upstream groundwater suggests that the reduction of NO^3-N concentration in the SGD can be attributed to the denitrification process. The denitrification occurred in the SGD, however, it was not observed in the Mn and Fe oxide reduction, and sulfate reduction reaction.

Figure 6 shows the water quality of SGD and upstream groundwater classified by a hexa-diagram. The result shows that the upstream groundwater at St.B is classified into semi-calcium bicarbonate type (Ca-HCO_3), which is generally seen in the deep aquifer. The groundwater at St.A and St.D was classified into non-sodium bicarbonate type (Na-HCO_3). In many cases, the SGD is easily classified into the Na-Cl type, because it often contains seawater and the Cl^- concentration is high. But, the SGD at the flood tide (FT) was classified into Na-HCO_3 type, because of Cl^- concentration of the sample is very low. Then, the SGD water is classified into Na-HCO_3 type, which is similar to the water type of the neighbouring shallow groundwater.

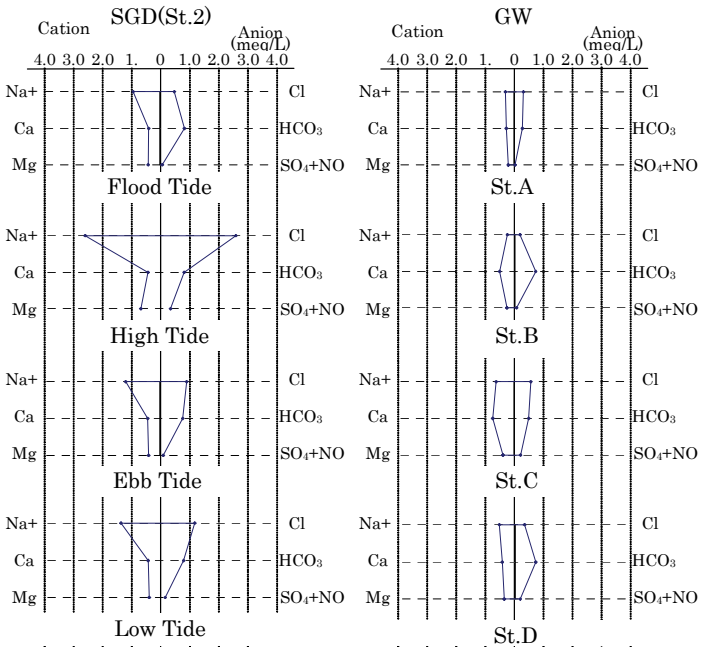

Fig. 6 Water quality classification by hexa-diagram.

Table 4 Nutrient loads at St.2.

Item	Concentration (mg/L)	SGD rate (μm/s)	Loads (g m^{-2} d^{-1})
TN	0.79	20.5	1.40
TP	0.04	20.5	0.07
SiO_2	29.8	205	52.78

Nutrient loads, such as TN, TP, SiO_2, in the SGD estimated at St.2 are presented in Table 4. These loads are larger than those found in previous investigations (Slomp & Van Cappellen, 2004). The average of molar ratio of TN and TP (N/P) in the SGD was 19.2 and this value is larger than the Radfield ratio (N/P = 16), and similar to that of general phytoplankton. As regards dissolved silicate, which is necessary for the proliferation of diatoms, the ratio of TN to DSi in the SGD (0.03) was lower than that in general phytoplankton (1.0). Therefore, the SGD in the study site has comparatively high dissolved DSi, and its value is favourable in terms of the growth of phytoplankton such as diatoms.

Figure 7 shows the relationship between hydrogen and oxygen stable isotopes (δD:$\delta^{18}O$) in the SGD of the upstream groundwater and seawater. The observed $\delta^{18}O$ in the sampling SGD indicated that SGD was formed by rain, which had fallen on the land at elevations below 300 m, according to the altitude effect in central Japan (Waseda *et al*., 1983). Geochemical tracer tests using the hydrogen and oxygen stable isotope ratio (δD:$\delta^{18}O$) indicated that SGD would be formed by the infiltrated rainwater at piedmont surface of low altitudes.

The groundwater discharge component of the watershed water budget in the Taradake area seems large, because the area consists of volcanic rocks with high permeability and low river baseflow rate. Therefore, a significant impact of the discharge through the SGD toward the Taradake sea area would be expected.

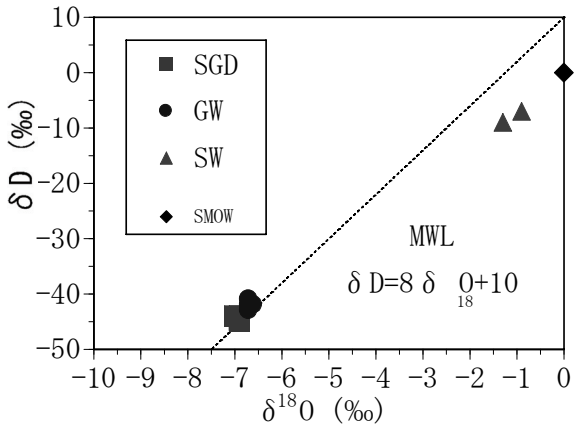

Fig. 7 Relationship between the hydrogen and oxygen stable isotopes (δD:δ^{18}O) in SGD (SMOW: standard mean ocean water, MWL: metric water line, Crage, 1961).

CONCLUSIONS

The present work is intended to take a first step at estimating nutrient inputs through SGD to Ariake Bay by measuring the inputs using a seepage meter. From the field measurements, it was shown that the SGD rate ranged from 0.01 to 20.52 μm/s at St.2. Water quality analyses indicated that SGD water was classified as semi-sodium bicarbonate type, which is similar to the neighbouring shallow groundwater. Moreover, denitrification is likely to be the reduction reaction process for SGD, while $Mn^{2+}$and Fe^{2+} oxide reduction and sulfate reduction are unlikely to proceed. Geochemical tracer tests using the hydrogen and oxygen stable isotope ratio (δD:δ^{18}O) indicated that SGD would be formed by the infiltrated rainwater at the piedmont surface of low altitudes, below 300 m. The SGD is likely to have been formed through locally developed cracks in an offshore submarine aquiclude from a shallow confined aquifer, consisting of pervious rock (basalt) and aquiclude (pyroclastic rock) with shorter residence time. Observed nutrient loads at the St.2 site have high values compared to previous investigations results. Therefore, the SGD found in the area would be a significant source of nutrients to the coastal sea area in Ariake Bay.

Hydrogeological maps and land-use maps in the catchment area of the Ariake Bay are to be compiled in the near future. In addition, a water balance model based on the quasi-3D freshwater–saltwater interface model, incorporating groundwater recharge, will be constructed.

Acknowledgements This research has been supported by Japan Science and Technology Agency.

REFERENCES

Crage, H. (1961) Isotopic variations in meteoric waters. *Science* **133**, 1702–1703.

Hill, A. R., Devito, K. J., Campangnolo, S. & Sanmugadas, K. (2000) Subsurface denitrification in a forest riparian zone: interactions between hydrology and supplies of nitrate and organic carbon. *Biogeochem.* **51**, 193–223.

Lee, D. R. (1977) A device for measuring seepage flux in lake and estuaries. *Limnol. Oceanogr*. **22**, 140–147.

Lovely, D. R. & Chapelle, F. H. (1995) Deep subsurface microbial processes. *Rev. Geophys.* **33**, 365–381.

Murphy, E. M. & Schramke, J. A. (1998) Estimation of microbial respiration rates in groundwater by geochemical modeling constrained with stable isotopes. *Geochim. Cosmochim. Acta* **62**(21/22), 3395–3406.

Slomp, C. P. & Van Cappellen, P. (2004) Nutrient inputs to the coastal ocean through submarine groundwater discharge: controls and potential impact. *J. Hydrol.* **295**, 64–86.

Taniguchi, M., Burnett, W. C., Cable, J. E. & Turner, J. V. (2002) Investigation of submarine groundwater discharge. *Hydrol. Processes* **16**, 2115–2129.

Waseda, A. & Nakai, N. (1983) Isotope composition of natural water in central Japan and Tohoku, Japan. *J. Geochem. Soc. Japan* **17**, 83–91.